Assessment of the fatigue transformation zone in bulk metallic glasses using positron annihilation spectroscopy

M. Liu,[1] R. S. Vallery,[1] D. W. Gidley,[1] M. E. Launey,[2] and J. J. Kruzic[3,a)]
[1]*Department of Physics, Randall Laboratory, University of Michigan, Ann Arbor, Michigan 48109, USA*
[2]*Materials Sciences Division, Lawrence Berkeley National Laboratory, Berkeley, California 94720, USA*
[3]*Materials Science, School of Mechanical, Industrial, and Manufacturing Engineering, Oregon State University, Corvallis, Oregon 97331, USA*

(Received 21 November 2008; accepted 23 March 2009; published online 1 May 2009)

Depth-profiled Doppler broadening spectroscopy of positron annihilation on fatigue fracture surfaces of two amorphous $Zr_{44}Ti_{11}Ni_{10}Cu_{10}Be_{25}$ metallic glass specimens reveals the presence of a layer of increased free volume induced by cyclic deformation, as compared to surfaces that have been etched to remove any surface damage. The damage layer, or *fatigue transformation zone* (FTZ), is generated by the propagating fatigue crack tip and the deduced size of that zone is similar to the predicted cyclic plastic zone size at a number of locations where the crack grew at different stress intensities. The presence of the FTZ is independent of the initial amount of bulk free volume, which was varied between the two specimens by structural relaxation via annealing, and the free volume sites generated in the zone are distinct from those typical of the bulk, as evidenced by the higher *S* parameter. Such observations support the concept that the mechanically induced free volume within the FTZ zone controls the fatigue crack growth rates rather than the initial free volume of the bulk material. © *2009 American Institute of Physics*. [DOI: 10.1063/1.3120784]

I. INTRODUCTION

Bulk metallic glasses (BMGs) are a relatively new class of engineering materials with unique and unusual properties that make them potential candidates for many structural applications.[1] Favorable properties include near theoretical strengths combined with reasonable fracture toughness, low damping, large elastic strain limits, and the ability to be thermoplastically formed into precision shaped parts with complex geometries,[2,3] all of which are generally distinct from, or superior to, corresponding crystalline metals and alloys. One property which has been perceived as a limitation for BMGs has been low fatigue resistance relative to crystalline metallic materials; however, not all studies to date have been in agreement with this point. For the most studied BMG, $Zr_{41.25}Ti_{13.75}Ni_{10}Cu_{12.5}Be_{22.5}$,[4] the reported 10^7 cycle fatigue strengths vary by a factor of 7,[5,6] and fatigue thresholds vary by a factor of three.[5] While some of the reported scatter may be explained by different testing configurations,[7] this does not account for all the observed variations, for example, those within single studies.[5,8] Results on crack initiation have also varied widely, with some published reports indicating almost immediate crack initiation at the onset of cycling,[9] while other results show a significant part of the fatigue life can be spent initiating a crack for a different BMG with similar composition.[10] Clearly there is a need for more fundamental understanding of fatigue mechanisms and the factors that govern fatigue behavior.

It is now widely accepted that metallic glasses are dense, more or less random arrangements of efficiently packed clusters of various atoms with different sizes, often exhibiting well-defined medium range order (MRO) on a scale of 1–2 nm.[11–14] Like crystalline metals, fatigue crack growth in BMGs is known to be governed by plastic deformation at the crack tip.[10,15,16] Spaepen originally proposed that the plastic deformation of metallic glasses utilizes rearrangement of atoms and free volume regions, where the free volume is the atomic volume in excess of the ideal densely packed but still amorphous structure.[17] Furthermore, inhomogeneous deformation is accommodated by the creation of additional free volume via a mechanism of flow-induced dilatation, which causes shear softening.[17] Experimental assessments of excess volume by positron annihilation spectroscopy[18,19] (PAS) and x-ray synchrotron radiation[20] provided evidence of such deformation-induced dilatation. Macroscopic deformation occurs within shear bands that are thought to initiate by the cooperative reorganization of atomic regions that involve tens of atoms referred to as shear transformation zones (STZs).[21–23] The plastic deformation response is therefore expected to depend on the initial state of the STZs, i.e., the initial local MRO and free volume.[24] As such, the amount of free volume has been shown to affect the deformation and fracture behavior of BMGs,[10,25–27] and recent studies demonstrated a pronounced effect on the fatigue life.[8,10] Surprisingly, one mechanical property, namely, the fatigue crack growth, has been found to be largely *unaffected* by bulk free volume differences.[10]

Because deformation of metallic glasses is accommodated by plastic rearrangement of STZs,[21] it may be expected that the intense deformation near a fatigue crack tip will generate a local increase in free volume. It has been proposed that this deformation induced free volume determines the local flow properties, rendering fatigue crack growth be-

a)Author to whom correspondence should be addressed. Tel.: +1-541-737-7027. FAX: +1-541-737-2600. Electronic mail: jamie.kruzic@oregonstate.edu.

havior relatively insensitive to initial bulk free volume differences.[10] PAS provides an experimental capability to examine subatomic open volumes and is therefore useful for directly analyzing the free volume in amorphous materials. Indeed, PAS has recently been used to demonstrate the presence of a *fatigue transformation zone* (FTZ) of enhanced free volume that is generated by a propagating fatigue crack tip.[28] Those results suggested that the zone of enhanced free volume is roughly equal in size to the extent of reversed plastic flow during each cycle, i.e., the cyclic plastic zone.[28] However, that initial study only looked at a single location on each sample and did not systematically characterize the extent of the FTZ over regions with different cyclic plastic zone sizes.

Accordingly, the purpose of this manuscript is to more fully characterize the FTZ, which forms during fatigue crack propagation in a Zr–Ti–Ni–Cu–Be based BMG. Specifically, by utilizing a focused positron beam, the Doppler broadening spectroscopy (DBS) technique of PAS is used to depth-profile fatigue fracture surfaces along several millimeters of crack growth to characterize the FTZ and its evolution during stable fatigue crack propagation.

II. EXPERIMENTAL METHODS

A. Materials

The two fully amorphous $Zr_{44}Ti_{11}Ni_{10}Cu_{10}Be_{25}$ compact tension C(T) specimens were heat treated differently to achieve residual stress free samples with different amounts of free volume prior to fatigue testing. The annealing procedures are described in detail elsewhere[10] and a brief description is given here. One sample was isothermally relaxed at 610 K for 10τ to lower the free volume relative to the as-cast condition, where τ represents the structural relaxation time (τ=438 s at 610 K).[29] After annealing for 10τ, the BMG was confirmed to be fully amorphous by high resolution transmission electron microscopy and is assumed to be fully relaxed into its metastable equilibrium, or lowest free volume state, with a normalized free volume difference relative to the original as cast state, $\Delta\nu_f/\nu_m$, of 0.044%.[29] Here $\Delta\nu_f$ is the average free volume difference per atom and ν_m is the atomic volume near the liquidus.[30] For the second sample, only a residual stress relief (SR) annealing treatment (573 K for 120 s) was applied and, unlike the 10τ sample, no free volume relaxation occurred due to the low temperature and short time, as confirmed by differential scanning calorimetry (DSC) experiments.[10]

In order to compare the PAS results for the FTZ to a nominally undeformed condition, two additional fatigue tested samples that were heat treated as described above were chemically etched using an acid solution ($HF:HNO_3:H_2O$=10:45:45 by volume) at 24 °C for 30 s to remove both the fatigue induced deformation on the fracture surfaces as well as the mechanical polishing damage on the polished surfaces. Roughly 10 μm of material was removed from the surfaces by etching. The etching procedure was found to be necessary as initial results indicated, in some cases, there is a surface damage layer associated with mechanical polishing that is smaller than, or similar in size to, that found on the fatigue fracture surfaces.[28]

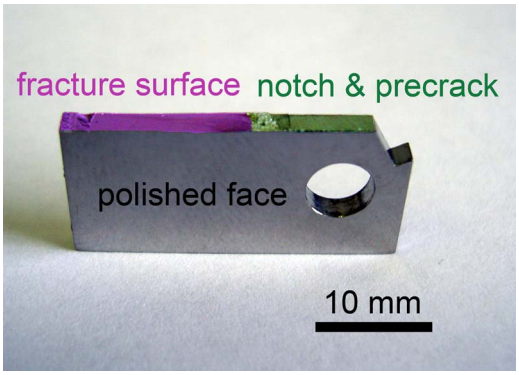

FIG. 1. (Color online) Typical half C(T) specimen after complete fatigue failure. Depth-profiled DBS experiments were performed on the polished face and the cyclically loaded fracture surface of the fatigue specimens. Some samples were examined after etching to remove any damage layers from fatigue or mechanical polishing.

B. Cyclic fatigue-crack growth rate measurements

Each C(T) sample was cycled until complete fatigue failure (Fig. 1). Fatigue crack growth experiments were conducted in general accordance with ASTM standard E647 (Ref. 31) using a computer controlled servohydraulic test machine with a frequency ν of 25 Hz (sine wave) and a constant load ratio (ratio of minimum to maximum applied load, $R=P_{min}/P_{max}$) of 0.1. The C(T) samples were of standard dimensions with thicknesses B=2.2 mm and width W=25.4 mm. Fatigue crack growth rates da/dN were measured as a function of the applied stress intensity range, $\Delta K=K_{max}-K_{min}$, where K_{max} and K_{min} are the maximum and minimum stress intensity experienced during the loading cycle. After complete sample fracture, free volume was characterized along the cyclically deformed fracture surfaces where the maximum applied stress intensity K_{max} ranged from ~3.2 to ~1.6 MPa$\sqrt{m}$. The gradient of applied stress intensities was achieved by growing the fatigue cracks under decreasing ΔK loading conditions with a normalized ΔK-gradient, $d\Delta K/da/d\Delta K$, of −0.08 mm^{-1}.[31]

C. Bulk positron annihilation lifetime spectroscopy

To better understand the size distribution of free volume voids in the bulk of the SR and 10τ samples, positron annihilation lifetime spectroscopy (PALS) was performed on each of them far away from the fracture surface. A small drop of radioactive ^{22}Na in saline solution was deposited and allowed to dry at the center of a polished face. The corresponding second half piece was placed over this insuring that all the beta-decay positrons from the source stop in the bulk of the sample (the positrons will penetrate only 0.1–0.2 mm deep). This sample-source sandwich arrangement was placed in a typical fast-timing PALS spectrometer with time resolution of 270 ps. Typically 4–10 million events were collected in each lifetime histogram. Standard lifetime fitting

programs were used to fit the lifetime spectrum to three lifetime components, which correspond to three different sizes of open volume voids (to be discussed).[32]

D. Depth-profiled Doppler broadening spectroscopy

DBS of positron annihilation is a standard positron annihilation spectroscopic technique to characterize the free volume defects and voids in materials. DBS monitors the energy spectrum of the annihilation radiation in a high energy resolution Ge gamma ray detector. The Doppler shifts in the 511 keV annihilation radiation resulting from the momentum of the annihilating positron-electron pair is manifested in the spectrum as a Doppler energy broadening of the 511 keV peak. The broadening of the 511 keV annihilation peak is characterized by the S parameter: the ratio of the number of counts within a central region of the peak to the total number of counts in the full peak. In this experiment, this central peak region for all DBS energy spectra was set to be between 0.88 keV above and below the 511 keV peak, a region which gave a fitted S parameter of nominally 0.5. Positron beams with variable positron implantation energies E in the range 1–10 keV can depth profile the defect characteristics up to several hundreds of nanometers below a BMG surface where significant deviations from bulk behavior may occur. The mean positron implantation depth for a normal incidence beam on a BMG with nominal density of 6 g/cm^3 is $\bar{z}(\mathrm{nm})=6.7[E(\mathrm{keV})]^{1.6}$. Details of depth-profiled PAS can be found elsewhere.[33–35]

In the present experiment, a focused positron beam with an on-target diameter of <2 mm was used to depth profile and compare both the deformed fracture surfaces and the polished faces of the two specimen types, SR and 10τ, before and after etching. As mentioned previously, the etched samples were free of any fatigue induced or mechanical polishing damage, hence, they were used as baselines for our experiments. Beam-based DBS experiments were conducted at a series of positions where the crack grew at different stress intensities (nominally 2 mm apart, see Fig. 1) along the deformed fracture edges (2.2 mm thick) of both SR and 10τ samples. The two fractured pieces of each sample were stacked side-by-side with their corresponding fracture edges aligned to give a total width of 4.4 mm, ensuring that no positrons missed the fracture surface. At each position along the fracture, a series of positron beam energies, from 1.1 to 10 keV, were used in order to profile the free volume variations from depths of ~8 to ~270 nm. On the etched samples, one central position ($x=8$ mm from left edge in Fig. 1) on the fatigue fracture surface was depth profiled by DBS for comparison along with the polished and etched side face (Fig. 1).

III. RESULTS

The fatigue crack-growth rates are found to be insensitive to free volume variations (Fig. 2). Here the results are presented in terms of the maximum stress intensity of the loading cycle K_{max} rather than the traditional stress intensity

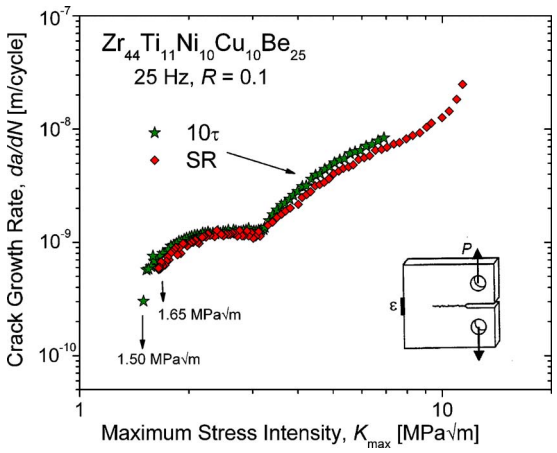

FIG. 2. (Color online) Fatigue crack-growth rates, da/dN, plotted as a function of the maximum applied stress intensity, K_{max}, for two different free volume states of $Zr_{44}Ti_{11}Ni_{10}Cu_{10}Be_{25}$.

range ΔK since the former corresponds with the maximum extent to the plastic deformation zone, as will be discussed below.

The bulk PALS results for both the 10τ and SR samples are identical. Consistent with Ref. 32, three lifetime components were fitted: a short 177.1 ± 0.4 ps lifetime with which 98.4% of the positrons annihilate, an intermediate lifetime of 420 ± 15 ps with 1.4% intensity, and a long 2.1 ± 0.2 ns lifetime with only 0.2%. This almost complete dearth of annihilation from the two longer lifetimes indicates they are essentially free of deformation induced flow defects and nanovoids.[32] The difference in free volume between the two samples is indistinguishable in PALS because it apparently just involves differences in concentrations of the smallest voids from which virtually all the positrons annihilate regardless of concentration.

The S parameters deduced from the depth-profiled DBS experiments were recorded as a function of mean positron implantation depth. In Fig. 3, the S parameter depth profiles at three different positions along the fatigue crack of the SR sample are shown (the same procedures were used on the 10τ sample and the detailed depth profiles are not shown here for clarity). For comparison, the S parameters for the polished and etched surface and etched fatigue fracture surface (at $x=8$ mm) are shown. These etched surface S parameters have been shifted by -0.011 and -0.007, respectively, since these data were acquired subsequent to an apparent shift in the gamma detector's energy resolution. More importantly and contrary to all the fractured surface depth profiles, the etched surfaces show no indication of an increased S parameter at low implantation depth. Indeed, there is a clear surface effect at depths less than 50 nm that is considerably more pronounced than the corresponding surface effect on the fractured surfaces. This is not surprising as the sample surface may be chemically altered by etching and the positron diffusion length in the fractured sample may be reduced by defect trapping, hence reducing the depth from which positrons can return to annihilate near the surface.

The fracture surface depth profiles were fit to a two layer model, ignoring data below 20 nm mean implantation depth

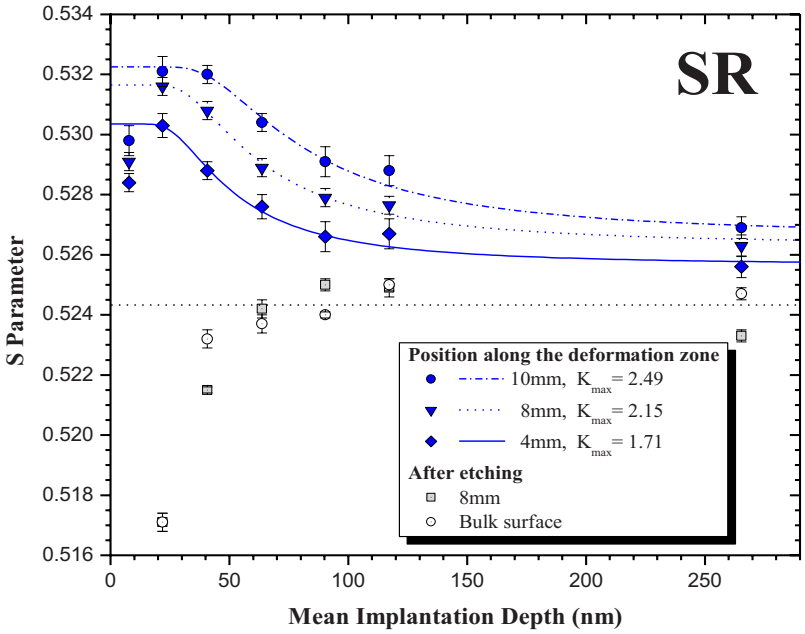

FIG. 3. (Color online) S parameter profiles and two-layer model fits of selected positions along the fatigue deformation zone of sample SR. The higher S parameters correspond to increased free volume induced by fatigue. Distances corresponding to each curve are measured from the left edge of the sample in Fig. 1 and each corresponds to a location where the fatigue crack was grown at a different stress intensity K_{max}. The stress intensity values are also given for each position (in MPa$\sqrt{m}$). Results for 10τ are similar to those shown above.

as being too strongly affected by an uninteresting surface state. In this simple model, a deformed region, i.e., the FTZ, with a uniformly higher S parameter due to annihilation in larger open volume fracture-induced defects is assumed to exist on top of an unaffected bulk region with a lower S parameter (as shown by PALS the bulk is quite free of deformation-induced defects). The observed S parameter is assumed to be an average of the two S parameters weighted by the fraction of positrons stopping in each layer (FTZ or bulk) as determined from the positron implantation profile.[33–35] Positron diffusion after implantation is taken to be negligible. The fitted parameters are the corresponding S parameters of the FTZ and in the bulk along with the depth/thickness of the transformation zone. Ideally, the bulk S parameters would be identical for each case, but minor differences in positron backscattering and detector resolution cause small variations that can be accounted for by fitting this bulk S value for each profile. The results of fitting to the two-layer model are shown in Fig. 3. The fitted values of the FTZ thickness at each location along the fracture surface for each sample is then plotted in Fig. 4 versus the calculated maximum stress intensity K_{max} at that specific location (to be discussed below).

IV. DISCUSSION

To explain the insensitivity of fatigue crack growth rates to the bulk free volume of the BMG, it has been proposed that the large cyclic plastic strains that occur near a fatigue crack tip cause a local increase in free volume, or FTZ.[10,28] Propagation of the crack requires it to grow through the zone of enhanced free volume and as such the local deformation properties are governed by the free volume within that zone rather than the bulk free volume of the material determined by the thermal history.

This theory predicts the depth of the fatigue-induced transformation layer should correspond with the expected extent of plastic deformation due to cyclic loading, i.e., the

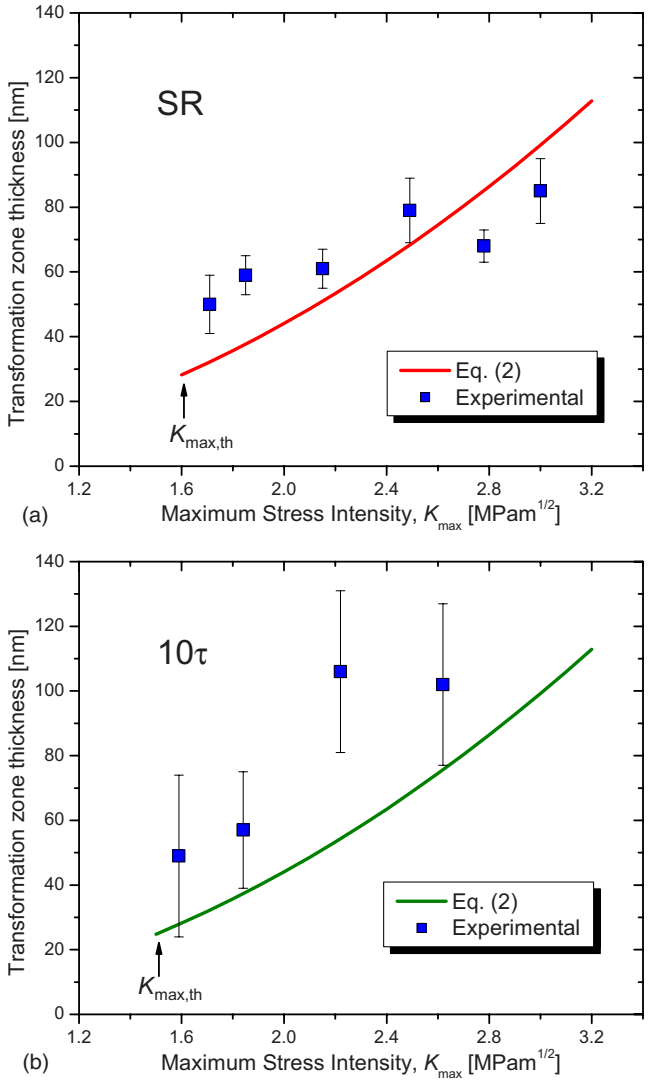

FIG. 4. (Color online) Thickness of the FTZ plotted as a function of the maximum stress intensity K_{max} for (a) the stress relieved sample SR (as-processed free volume), and (b) the sample 10τ (relaxed lower free volume state). Reasonable correlations are found between the experimental data from depth-profiled DBS experiments and the theoretical estimate defined by Eq. (2).

FTZ size should increase with increasing stress intensity. This is clearly confirmed by the results in Fig. 4, where both samples show a trend of increasing FTZ size with increasing stress intensity. Furthermore, it is interesting to compare the PAS measured FTZ thicknesses to plastic zone size estimates from linear elastic fracture mechanics. For plane strain conditions, the overall plastic zone extent normal to the crack plane (i.e., into the fracture surface) is roughly three times that in the direction ahead of the crack tip, i.e.,[36]

$$r_p = \frac{1}{2\pi}\left(\frac{K_{\max}}{\sigma_Y}\right)^2, \tag{1}$$

where $K_{\max}$ is the maximum stress intensity of the loading cycle and σ_Y is the yield stress of the material ($\sim$1900 MPa).[37] During cyclic loading, there is a smaller cyclic plastic zone where reversed plastic flow occurs during each cycle. It is generally accepted that this cyclic plastic zone is roughly $\frac{1}{4}$ the total plastic zone size.[38] This would predict the depth of the FTZ into each fracture surface to correspond roughly to

$$r_{\mathrm{FTZ}} = \frac{1}{8\pi}\left(\frac{K_{\max}}{\sigma_Y}\right)^2. \tag{2}$$

This concept is indeed consistent with the DBS results. Figure 4 shows Eq. (2) (with no fitted parameters) plotted along with the depth profiled DBS results and the agreement is quite reasonable. The present theory catches the key features associated with the FTZ formation: (i) fatigue cycling induces a FTZ ahead of the crack tip that has distinctly larger free volume voids than the bulk and (ii) the thickness of the FTZ is roughly similar to the expected cyclic plastic zone. Furthermore, such results help explain the surprising insensitivity of fatigue crack growth rates to the initial free volume of the BMG. Indeed, the local free volume appears to be determined by the cyclic deformation rather than the thermal history.

There are some discrepancies between the data and predictions that should be discussed, however, such as the fact that the DBS measured data do not appear to rise as fast with the stress intensity as the prediction does for the SR sample in Fig. 4(a) and the zone size is somewhat under predicted for the 10τ sample in Fig. 4(b). Here it is important to note some limitations of the present analysis. First, to minimize the number of fitted parameters, the two layer model used to determine the layer thickness values assumed the FTZ layers to have a constant S parameter, when in fact it is likely graded from a peak value near the surface to a value closer to the bulk near the interface. Second, the traditional fracture mechanics methods for determining plastic zone sizes have all been developed for crystalline metals. There are several mechanistic differences in the plastic flow behavior of crystalline versus amorphous metals. While crystalline metals deform by dislocation motion at constant volume, usually accompanied by strain hardening, amorphous metals deform at low temperatures by highly localized flow in shear bands with locally increasing volume and strain softening. Finally, the plastic zone is affected by the constraint of the surrounding elastic material and in this case there are distinct differences in the surrounding elastic materials due to the different heat treatments. This latter factor could help explain why agreement appears to be better in the SR case than the 10τ case. Thus, while the key features of the theory are captured in the present work, there is clearly more work to be done to fully understand the cyclic plastic zone formed in amorphous metals.

While it appears that the expected size of the FTZ is nominally described by Eq. (2), less is known about the internal structure. As mentioned earlier, recent PALS and DBS results suggest that the size distribution of free volume sites may be trimodal.[32] Indeed, three characteristic positron lifetimes have been observed suggesting three distinct size ranges for free volume elements. The smallest free volume size corresponds to Bernal holes (tetrahedral interstitial holes) in the densely packed structure. Bernal holes are intrinsic to the glassy structure and cannot relax out completely with annealing. The intermediate size corresponds to larger flow defects, while the longest lifetime corresponds to the lifetime of orthopositronium in nanovoids with radii of a few angstroms.[32] The average size of the small and intermediate sized sites is thought to decrease with extensive deformation, while the largest sites remain roughly constant in size. Also, the concentrations of the larger two sites increase with large deformations at the expense of the smallest sites.[32]

In the present experiments, both bulk PALS and depth profiled DBS are not sensitive to the free volume changes from structural relaxation. For the latter case, the depth profiled data asymptotes to roughly the same value of the S parameter in both the 10τ and SR cases. This suggests that every positron is finding a free volume element to trap in and free volume changes due to structural relaxation do not significantly change the size of those free volume elements. Using atomic models of amorphous Pd–Ni–P, Sietsma and Thijsse[39] addressed the effect of structural relaxation on the volume distribution of the free volume elements. They found that the difference between as-quenched and annealed BMG predominantly lies in the quantity of the flow defects. More specifically, the number of intrinsic voids, or Bernal holes, increases, whereas the number of flow defects decreases after annealing. The interpretation is that during structural relaxation the flow defects break up into two or more Bernal holes. Therefore, it is unlikely that a high concentration of flow defects and nanovoids would exist in the glass after extensive structural relaxation. This is completely consistent with our PALS data. Accordingly, structural relaxation appears to affect the concentration of the smallest free volume elements (Bernal holes), rather than the size, while cyclic deformation produces distinctly larger free volume sites, as evidenced by the higher S values.

V. CONCLUSIONS

Based on depth profiled PAS results characterizing multiple positions along the fatigue fracture surfaces for a Zr–Ti–Ni–Cu–Be BMG, the following conclusions can be made:

(1) The existence of a layer of locally increased free volume, i.e., a fatigue transformation zone (FTZ), is confirmed at every point observed along the fatigue fracture

surfaces. Indeed, when compared to the depth profile for an undeformed etched surface, the fatigue fracture surface shows a distinctly higher *S* parameter, which decreases asymptotically with depth to the nominal bulk value.

(2) The increased free volume of the FTZ almost certainly is comprised of larger flow defects and/or nanovoids. PALS results conclusively show that very few of these larger voids exist in the undeformed bulk state of either sample. Since DBS is found to be insensitive to differing concentrations of the smallest, intrinsic voids (Bernal holes) it is concluded that larger defects are responsible for the increased *S* parameter in the FTZ. Future measurements with high time resolution depth-profiled PALS could confirm this deduction.

(3) By fitting the depth profiled *S* parameter data to a simple two layer model, it was found that the deduced size of the FTZ corresponds reasonably well with estimates of the cyclic plastic zone size from linear elastic fracture mechanics. A trend of increasing zone size with increasing maximum stress intensity is clearly seen, which is roughly equal to that predicted based on a simple estimate of the variation in the cyclic plastic zone size; however, future work is likely needed to understand all of the details involved in the cyclic plastic zone formation in metallic glasses.

ACKNOWLEDGMENTS

M.E.L. and J.J.K. thank Dr. A. Peker and Dr. J. Schroers for supplying the material and Dr. R. Busch for many useful discussions. D.W.G. gratefully acknowledges the support of the University of Michigan for positron research.

[1]C. J. Byrne and M. Eldrup, Science **321**, 502 (2008).
[2]M. F. Ashby and A. L. Greer, Scr. Mater. **54**, 321 (2006).
[3]J. Schroers, JOM **57**, 35 (2005).
[4]All compositions are given in terms of at. %.
[5]C. J. Gilbert, J. M. Lippmann, and R. O. Ritchie, Scr. Mater. **38**, 537 (1998).
[6]G. Y. Wang, P. K. Liaw, A. Peker, B. Yang, M. L. Benson, W. Yuan, W. H. Peter, L. Huang, M. Freels, R. A. Buchanan, C. T. Liu, and C. R. Brooks, Intermetallics **13**, 429 (2005).
[7]B. C. Menzel and R. H. Dauskardt, Scr. Mater. **55**, 601 (2006).
[8]M. E. Launey, R. Busch, and J. J. Kruzic, Scr. Mater. **54**, 483 (2006).
[9]B. C. Menzel and R. H. Dauskardt, Acta Mater. **54**, 935 (2006).
[10]M. E. Launey, R. Busch, and J. J. Kruzic, Acta Mater. **56**, 500 (2008).
[11]D. B. Miracle, Nature Mater. **3**, 697 (2004).
[12]A. R. Yavari, Nature (London) **439**, 405 (2006).
[13]H. W. Sheng, W. K. Luo, F. M. Alamgir, J. M. Bai, and E. Ma, Nature (London) **439**, 419 (2006).
[14]T. Egami, Intermetallics **14**, 882 (2006).
[15]C. J. Gilbert, R. O. Ritchie, and W. L. Johnson, Appl. Phys. Lett. **71**, 476 (1997).
[16]C. J. Gilbert, V. Schroeder, and R. O. Ritchie, Metall. Mater. Trans. A **30**, 1739 (1999).
[17]F. Spaepen, Acta Metall. **25**, 407 (1977).
[18]K. M. Flores, D. Suh, R. H. Dauskardt, P. Asoka-Kumar, P. A. Sterne, and R. H. Howell, J. Mater. Res. **17**, 1153 (2002).
[19]B. P. Kanungo, S. C. Glade, P. Asoka-Kumar, and K. M. Flores, Intermetallics **12**, 1073 (2004).
[20]K. Hajlaoui, T. Benameur, G. Vaughan, and A. R. Yavari, Scr. Mater. **51**, 843 (2004).
[21]A. S. Argon, Acta Metall. **27**, 47 (1979).
[22]C. A. Schuh and A. C. Lund, Nature Mater. **2**, 449 (2003).
[23]M. L. Falk and J. S. Langer, Phys. Rev. E **57**, 7192 (1998).
[24]D. B. Miracle, T. Egami, K. M. Flores, and K. F. Kelton, MRS Bull. **32**, 629 (2007).
[25]R. Gerling, F. P. Schimansky, and R. Wagner, Acta Metall. **36**, 575 (1988).
[26]J. J. Lewandowski, W. H. Wang, and A. L. Greer, Philos. Mag. Lett. **85**, 77 (2005).
[27]P. Murali and U. Ramamurty, Acta Mater. **53**, 1467 (2005).
[28]R. S. Vallery, M. Liu, D. W. Gidley, M. E. Launey, and J. J. Kruzic, Appl. Phys. Lett. **91**, 261908 (2007).
[29]M. E. Launey, J. J. Kruzic, C. Li, and R. Busch, Appl. Phys. Lett. **91**, 051913 (2007).
[30]K. Ohsaka, S. K. Chung, W. K. Rhim, A. Peker, D. Scruggs, and W. L. Johnson, Appl. Phys. Lett. **70**, 726 (1997).
[31]*Metals-Mechanical Testing; Elevated and Low-temperature Tests; Metallography*, Annual Book of ASTM Standards Vol. 03.01 (ASTM International, West Conshohocken, Pennsylvania, 2005).
[32]K. M. Flores, E. Sherer, A. Bharathula, H. Chen, and Y. C. Jean, Acta Mater. **55**, 3403 (2007).
[33]P. J. Schultz and K. G. Lynn, Rev. Mod. Phys. **60**, 701 (1988).
[34]P. G. Coleman, *Positron Beams and Their Applications* (World Scientific, Singapore, 2000).
[35]D. W. Gidley, H. G. Peng, and R. S. Vallery, Annu. Rev. Mater. Res. **36**, 49 (2006).
[36]T. L. Anderson, *Fracture Mechanics: Fundamentals and Applications*, 3rd ed. (Taylor and Francis, Boca Raton, FL, 2005).
[37]H. A. Bruck, T. Christman, A. J. Rosakis, and W. L. Johnson, Scr. Metall. Mater. **30**, 429 (1994).
[38]J. R. Rice, *Fatigue Crack Propagation* (ASTM, Philadelphia, PA, 1967), p. 417.
[39]J. Sietsma and B. J. Thijsse, Phys. Rev. B **52**, 3248 (1995).